(Preprint) AAS XX-XXX

SUN-AVOIDANCE SLEW PLANNING ALGORITHM WITH POINTING AND ACTUATOR CONSTRAINTS

Mohammad Ayoubi[*] and Junette Hsin[†]

A novel geometric approach for a sun (or any bright object) avoidance slew maneuver with pointing and actuator constraints is presented. We assume spacecraft has a single light-sensitive payload with control-torque and reaction wheels' angular momentum constraints. Furthermore, we assume the initial and final attitudes, instrument boresight vector, and sun vector are known. Then we use Pontryagin's minimum principle (PMP) and derive the desired or target-frame quaternions, angular velocity and acceleration for two cases: 1) with control-torque and reaction wheels' angular momentum constraints, and 2) with control-torque. constraint. In the end, a Monte Carlo simulation is performed to show the viability of the proposed algorithm with control-torque and angular momentum constraints.

INTRODUCTION

Large-angle slew maneuvers are required during any Earth-pointing or interplanetary missions. In many space missions, and for safety consideration, a sensitive payload such as imaging camera or telescope needs to be retargeted while avoiding sun vector or other bright objects in the sky. The attitude reorientation problem in the presence of attitude constrained zones has been studied in the last three decades. McInnes[1] addressed this problem via using an artificial potential function. He proposed a guidance law which is entirely analytical and suitable for onboard implementation. However, he uses Euler angles which are singular for large slew angles. A geometric approach was proposed by Spindle,[2] Hablani,[3] and Biggs and Colley[4] where a feasible attitude maneuver, or a guidance law, is precomputed based on the attitude-avoidance-zone constraints. Another approach for addressing this problem is using randomized algorithms.[5] However, depends on the number of constraints and initial and final attitudes, this approach is computationally expensive and not suitable for onboard implementation. Another approach for solving the time optimal reorientation maneuver subject to boundaries and path constraints is proposed by Spiller et al.[6] They used the particle swarm optimization (PSO) technique to find a sub-optimal solution with keep-out constraints. Another approach is to cast the problem as a convex optimization problem and use a semi-definite programming (SDP) or quadratically constrained quadratic programming (QCQP) to solve them. See for instance Kim and Mesbahi,[7] Kim et al.,[8] Sun and Dai,[9] and Lee and Mesbahi.[10] Recently, Ramos and Schaub[11] proposed a method based on the Lyapunov stability theorem and logarithmic barrier potential function to derive a steering law for attitude control of a spacecraft subject to conically constrained inclusion and exclusion regions. They also considered the control-torque constraint in their algorithm.

[*]Associate Professor, Department of Mechanical Engineering, Santa Clara University, Santa Clara, CA 95053. AIAA senior member, AAS senior member.

[†]Engineer, Dynamics and Control Analysis Group, Space Solutions (formerly Space Systems/Loral), postal address.

In this paper, we present a novel geometric approach for large-angle slew planning with pointing and actuator constraints. We assume spacecraft has a single light-sensitive payload with control-torque and reaction wheels' angular momentum constraints. Furthermore, we assume the initial and final attitudes, instrument boresight vector, and sun vector are known. Then we derive the desired or target-frame quaternions, angular velocity, and angular acceleration based on the Pontryagin's minimum principle (PMP) for the proposed maneuver. The proposed algorithm in this paper is intuitive, deterministic, easy to implement, and includes the control-torque and reaction wheels' angular momentum constraints. The main drawback of the proposed algorithm is its limitation for a single sensitive-payload. A Monte Carlo simulation is performed to show the viability of the proposed algorithm with control-torque and angular momentum constraints.

PROBLEM FORMULATION

Consider a gyrostat (a rigid body with reaction wheels) in a low earth orbit (LEO). Assume a newtonian frame, N, and a gyrostat-centered unit sphere frame G with a center G^* at the center-of-mass of the gyrostat as shown in Fig. 1. The sun or bright-object avoidance planning problem can be stated as follows: Assume the initial state, $x_i = \left[{}_{\mathcal{N}}\hat{P}_i, {}^{\mathcal{N}}_{\mathcal{G}}\omega^{\mathcal{G}}(t_i), {}^{\mathcal{N}}q^{\mathcal{G}}(t_i)\right] \in \mathbb{R}^3 \times \mathbb{R}^3 \times \mathbb{SO}(3)$, final state, $x_f = \left[{}_{\mathcal{N}}\hat{P}_f, {}^{\mathcal{N}}_{\mathcal{G}}\omega^{\mathcal{G}}(t_f), {}^{\mathcal{N}}q^{\mathcal{G}}(t_f)\right] \in \mathbb{R}^3 \times \mathbb{R}^3 \times \mathbb{SO}(3)$, the sun unit vector in the inertial frame,${}_{\mathcal{N}}\hat{S} \in \mathbb{R}^3$, the sensitive instrument boresight unit vector in the body-fixed frame, ${}_{\mathcal{G}}\hat{P} \in \mathbb{R}^3$, and the half-cone angle $\epsilon_p \in \mathbb{R}$ are given. Find: A sequence of slew maneuvers such that the sun vector does not enter into the on-board sensitive instrument forbidden cone for all times $t \in [t_i, t_f]$ subject to actuator constraints.

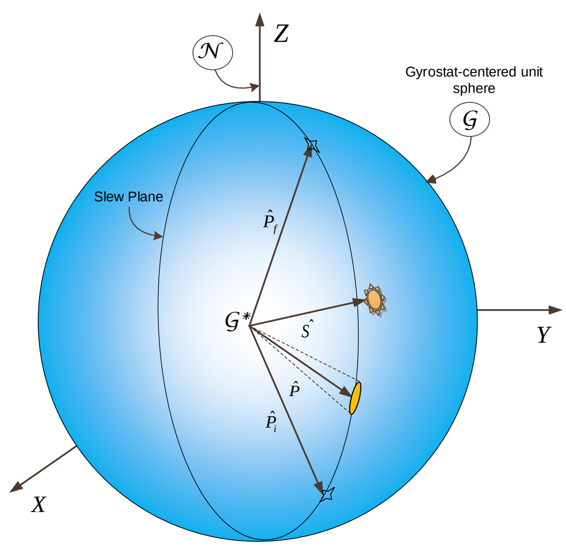

Figure 1. Gyrostat-centered unit sphere centered at point $\mathcal{G}^*$.

SUN-AVOIDANCE SLEW (SAS) ALGORITHM DESCRIPTION

The first step is to determine if there is a sun vector intrusion. To this end we check the angular separation, α, between the sun unit vector, ${}_{\mathcal{N}}\hat{S}$, and the $\hat{P}_i - \hat{P}_f$ plane or "slew plane."

$$\alpha = \frac{\pi}{2} - \cos^{-1}(\hat{S} \cdot \hat{e}) \tag{1}$$

where the eigenaxis unit vector is determined by

$$\hat{e} = \frac{\hat{P}_i \times \hat{P}_f}{|\hat{P}_i \times \hat{P}_f|} \tag{2}$$

If $|\alpha| >= \epsilon_p$ then the sun vector intrusion does not happened. Otherwise, we need to perform sun-avoidance slew maneuver which is explained in the next section.

Slew Planning If $|\alpha| < \epsilon_p$ then we need to plan the sun-avoidance slew in the following steps:

1. The 1^{st} slew is around the eigenaxis, $\hat{e}$, through angle ϕ_1:

$$\phi_1 = \begin{cases} \cos^{-1}(\hat{P} \cdot_{\mathcal{G}} \hat{S}_{||}) - \epsilon_p & when \ \cos^{-1}(\hat{P} \cdot_{\mathcal{G}} \hat{S}_{||}) - \epsilon_p \leq \pi \\ \cos^{-1}(\hat{P} \cdot_{\mathcal{G}} \hat{S}_{||}) - \epsilon_p - 2\pi & when \ \cos^{-1}(\hat{P} \cdot_{\mathcal{G}} \hat{S}_{||}) - \epsilon_p > \pi \end{cases} \tag{3}$$

where

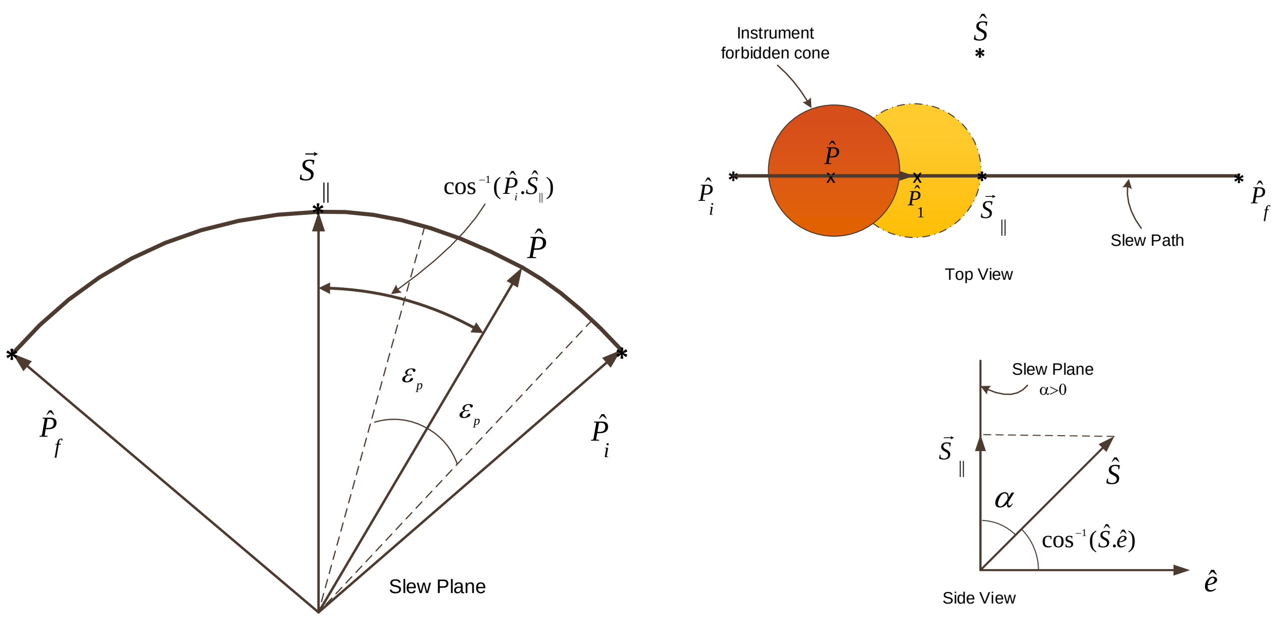

Figure 2. The sensitive instrument boresight vector motion during the 1^{st} slew.

$$\vec{S}_{||} = \hat{S}\cos\alpha. \tag{4}$$

Because It should be noted that the vector $\hat{S}_{||}$ is in the $\mathcal{N}$-frame, therefore it should be transformed in the $\mathcal{G}$-frame before it can be used in Eq. (3).

2. The 2^{nd} slew is around the unit sun vector, $\hat{S}$, via angle ϕ_2.

   (a) when $\alpha \neq 0$

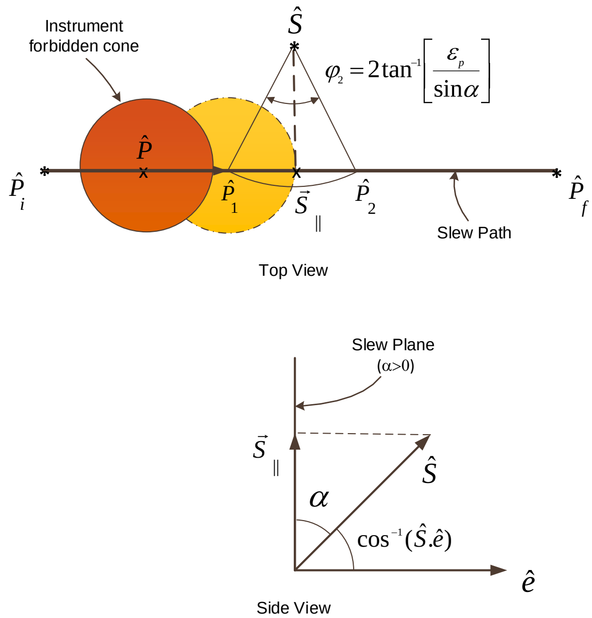

Figure 3. The sensitive instrument boresight vector motion during the 2^{nd} slew when $\alpha \neq 0$.

   (b) when $\alpha = 0$

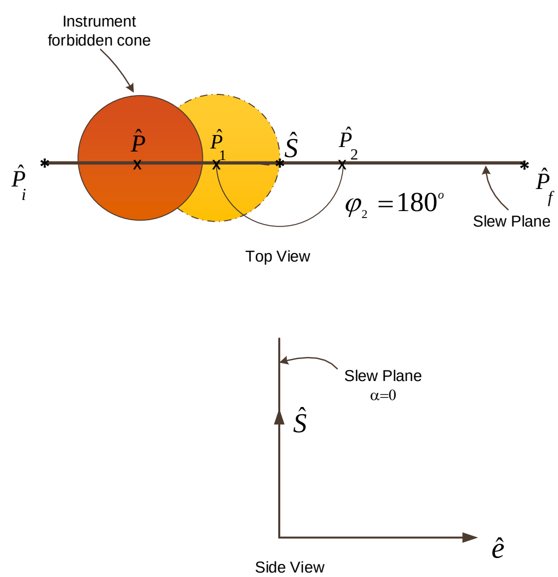

Figure 4. The sensitive instrument boresight vector motion during the 2^{nd} slew when $\alpha = 0$.

3. The 3^{rd} slew is about the $\hat{e}$ through angle ϕ_3:

$$\phi_3 = \begin{cases} \cos^{-1}({}_{\mathcal{G}}\hat{P}_f \cdot \hat{P}_2) & when\ {}_{\mathcal{G}}\hat{P}_f \cdot \hat{P}_2 \geq 0 \\ \cos^{-1}({}_{\mathcal{G}}\hat{P}_f \cdot \hat{P}_2) - 2\pi & when\ {}_{\mathcal{G}}\hat{P}_f \cdot \hat{P}_2 < 0 \end{cases} \tag{5}$$

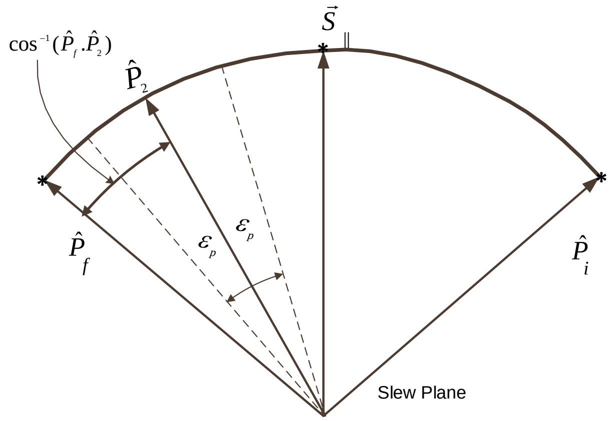

Figure 5. The sensitive instrument boresight vector motion during the 3^{rd} slew.

Similar to the 1^{st} maneuver, the vector ${}_{\mathcal{N}}\hat{P}_f$ needs to be transformed to the $\mathcal{G}$-frame before doing the dot product in Eq. (5).

4. The final slew about the instrument boresight axis may needed to go to the final attitude.

Summary of Algorithm

1. Slew around the eigenaxis,$\hat{e}$, through angle:

$$\phi_1 = \begin{cases} \cos^{-1}(\hat{P} \cdot_{\mathcal{G}} \hat{S}_{||}) - \epsilon_p & when\ \cos^{-1}(\hat{P} \cdot_{\mathcal{G}} \hat{S}_{||}) - \epsilon_p \leq \pi \\ \cos^{-1}(\hat{P} \cdot_{\mathcal{G}} \hat{S}_{||}) - \epsilon_p - 2\pi & when\ \cos^{-1}(\hat{P} \cdot_{\mathcal{G}} \hat{S}_{||}) - \epsilon_p > \pi \end{cases} \tag{6}$$

2. Slew around the $\hat{S}$ via:

$$\phi_2 = \begin{cases} 2\tan^{-1}(\frac{\epsilon_p}{\sin\alpha}) & when\ \alpha \neq 0 \\ \pi & when\ \alpha = 0 \end{cases} \tag{7}$$

3. Slew about the $\hat{e}$ through angle:

$$\phi_3 = \begin{cases} \cos^{-1}({}_{\mathcal{G}}\hat{P}_f \cdot \hat{P}_2) & when\ {}_{\mathcal{G}}\hat{P}_f \cdot \hat{P}_2 \geq 0 \\ \cos^{-1}({}_{\mathcal{G}}\hat{P}_f \cdot \hat{P}_2) - 2\pi & when\ {}_{\mathcal{G}}\hat{P}_f \cdot \hat{P}_2 < 0 \end{cases} \tag{8}$$

4. If necessary, Perform the final rotation, ϕ_4, about the instrument boresight axis to adjust the attitude.

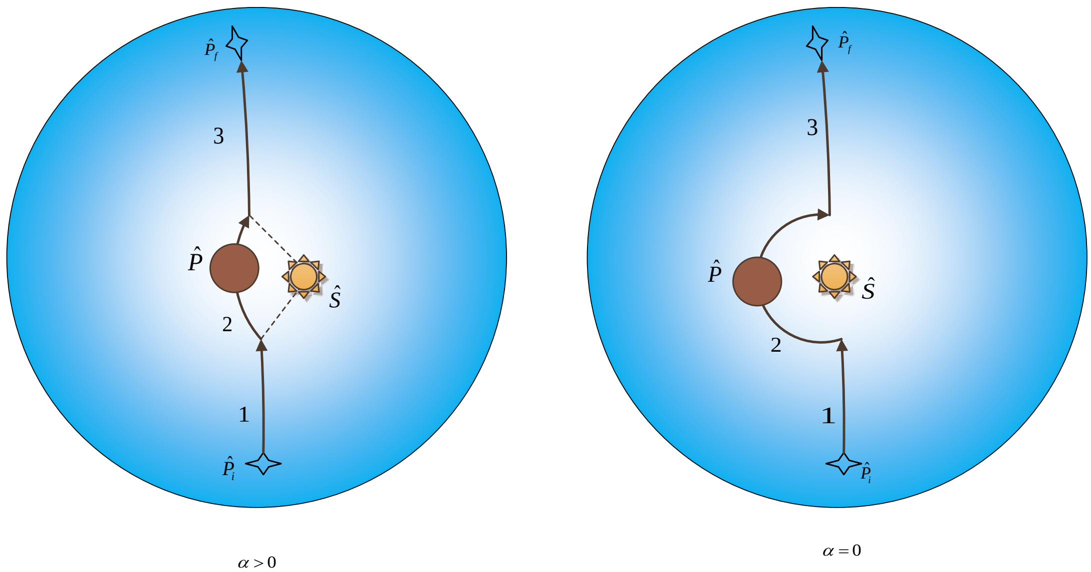

Figure 6. The trajectory of the instrument boresight tip on the gyrostat-centered unit sphere during the SAS maneuver.

STEERING LAWS

In this section we utilize the proposed sun-avoidance slew algorithm to generate the required angular rate, ${}^{\mathcal{N}}_{\mathcal{G}}\omega^{\mathcal{T}}$, angular acceleration, ${}^{\mathcal{N}}_{\mathcal{G}}\alpha^{\mathcal{T}}$, and quaternions, ${}^{\mathcal{N}}q^{\mathcal{T}}$, for the control system. Figure 7 shows how the generated commands is utilized by an attitude control system to guide the gyrostat in each leg of the SAS.

In the following, we formulate the problem of finding the steering laws for two cases with: 1) velocity and acceleration constraints and 2) acceleration constraint.

Case 1: Single-Axis, Agile Slew Maneuver with Velocity and Acceleration Constraints.

Problem Statement: Consider the motion of a gyrostat around a given inertially-fixed axis, ${}_{\mathcal{N}}\hat{e} = [e_x, e_y, e_z]^T$. The problem of minimum-time slew maneuver around the ${}_{\mathcal{N}}\hat{e}$ axis can be formulated as:

$$\underset{u}{Minimze}\ \mathcal{J}[x(.), u(.), t_f] = \int_{t0}^{t_f} dt, \tag{9}$$

subject to the following dynamic constraints:

$$\Sigma_{\mathcal{G}} : \begin{cases} \dot{x}_1 = x_2, \\ \dot{x}_2 = M/I_{\hat{e}}^{\mathcal{G}/\mathcal{G}*} = u, \end{cases} \tag{10}$$

where $x_1 \triangleq \phi$, $x_2 = \dot{\phi}$, M is the projection of the reaction wheel or other actuators torque along the $\hat{e}$, and

$$I_{\hat{e}}^{\mathcal{G}/\mathcal{G}*} = \hat{e}\, I^{\mathcal{G}/\mathcal{G}*}\, \hat{e}^T. \tag{11}$$

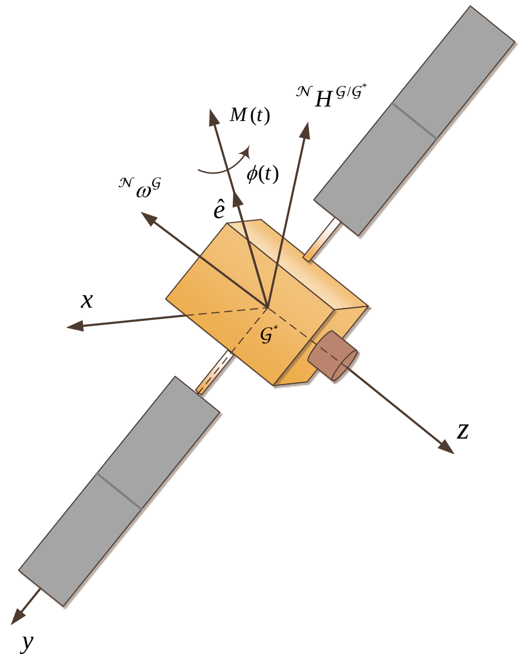

Figure 7. A gyrostat rotating about the eigenaxis, $\hat{e}$.

The boundary conditions are given by

$$BCs : \begin{cases} \phi(t_0) = 0, \phi(t_f) = \phi_f, \\ \dot{\phi}(t_0) = \dot{\phi}_0, \dot{\phi}(t_f) = \dot{\phi}_f, \end{cases} \tag{12}$$

and the reaction wheels' angular momentum and control-torque acceleration can be transformed into the angular velocity and angular acceleration constraints as follows

$$C_1 : \begin{cases} |x_2 = \dot{\phi}| \leq \dot{\phi}_{max}, \\ |u = \ddot{\phi}| \leq \ddot{\phi}_{max}, \end{cases} \tag{13}$$

in which

$$\dot{\phi}_{max} = [I^{w/w^*}]^{-1}[{}^{\mathcal{N}}H^{\mathcal{G}/\mathcal{G}*} - (I^{\mathcal{G}/\mathcal{G}*} + I^{w/w*})^{\mathcal{N}}\omega^{\mathcal{G}}]/(e_x + e_y + e_z), \tag{14}$$

and

$$\ddot{\phi}_{max} = M_{max}/I_{\hat{e}}^{\mathcal{G}/\mathcal{G}*}, \tag{15}$$

where ${}^{\mathcal{N}}H^{\mathcal{G}/\mathcal{G}*}$ is the total angular momentum of the gyrostat with respect to its center of mass, $\mathcal{G}^*$, in the $\mathcal{N}$-frame. $I^{\mathcal{G}/\mathcal{G}^*}$ and $I^{w/w*}$ represent the mass-moment-of-inertia of the gyrostat and reaction wheels with respect to their center of masses, respectively. M_{max} is the maximum available torque along the eigenaxis in the $\mathcal{G}$-frame. Find ${}^{\mathcal{N}}\omega^{\mathcal{T}}$, ${}^{\mathcal{N}}\alpha^{\mathcal{T}}$, and ${}^{\mathcal{N}}q^{\mathcal{T}}$.

Using the optimal control theory and Pontryagin's minimum principle (PMP), we derive the necessary conditions for the optimal solution as follows:

1. State Eqs.:

$$\begin{cases} \dot{x}_1 = x_2, \\ \dot{x}_2 = u, \\ \dot{x}_3 = (x_2 + \dot{\phi}_{max})^2 \mathbb{U}(-x_2 - \dot{\phi}_{max}) + (\dot{\phi}_{max} - x_2)^2 \mathbb{U}(x_2 - \dot{\phi}_{max}), \end{cases} \tag{16}$$

   where the unit step function, $\mathbb{U}$, is defined as

$$\mathbb{U}(X) = \begin{cases} 1, X > 0, \\ 0, X \leq 0. \end{cases} \tag{17}$$

   Note: $(x_3(t_0) = x_3(t_f) = 0$ & $x_3(t) \geq 0\ ) \rightarrow x_3(t) = 0, t \in [t_0, t_f]$.

2. Hamiltonian:

$$\begin{aligned} \mathscr{H} =& 1 + \lambda_1 x_2 + \lambda_2 u + \lambda_3 \Big[(x_2 + \dot{\phi}_{max})^2 \mathbb{U}(-x_2 - \dot{\phi}_{max}) \\ & (\dot{\phi}_{max} - x_2)^2 \mathbb{U}(x_2 - \dot{\phi}_{max}) \Big] \end{aligned} \tag{18}$$

3. Costate Eqs.:

$$\begin{cases} \dot{\lambda}_1 = -\frac{\partial \mathscr{H}}{\partial x_1} = 0, \\ \dot{\lambda}_2 = -\frac{\partial \mathscr{H}}{\partial x_2} = -\lambda_1 - 2\lambda_3 (x_2 + \dot{\phi}_{max}) \mathbb{U}(-x_2 - \dot{\phi}_{max}) \\ +2\lambda_3 (\dot{\phi}_{max} - x_2) \mathbb{U}(x_2 - \dot{\phi}_{max}), \\ \dot{\lambda}_3 = -\frac{\partial \mathscr{H}}{\partial x_3} = 0. \end{cases} \tag{19}$$

4. Applying the Pontryagin's minimum principle (PMP),

$$u^* = \underset{u \in \mathcal{U}}{argmin} \mathscr{H}, \tag{20}$$

   where $\mathcal{U}$ defines the domain of feasible controls. The optimal control can be determined as

$$u^*(t) = \begin{cases} \ddot{\phi}_{max} & \lambda_2 < 0, \\ ? & \lambda_2 = 0, \\ -\ddot{\phi}_{max} & \lambda_2 > 0. \end{cases} \tag{21}$$

   This is a *singular arc* optimal control problem.

5. Determining the optimal control in the singular arc:

$$\frac{d^2}{dt^2}\Big(\frac{\partial \mathscr{H}}{\partial u}\Big) = \ddot{\lambda}_2 = 0 \rightarrow \dot{x}_2 = 0 \rightarrow u^* = 0 \tag{22}$$

6. Checking the Generalized Legendre-Clebsch condition for optimality:

$$(-1)^2 \frac{\partial}{\partial u}\Big[\frac{d^2}{dt^2}\Big(\frac{\partial \mathscr{H}}{\partial u}\Big)\Big] = 1 \geq 0 \tag{23}$$

7. Checking the transversality condition:

$$\mathscr{H}|_{(*,t_f)} = 0 \text{ and } \mathscr{H} \neq \mathscr{H}(t) \rightarrow \mathscr{H} = 0, \forall t \in [t_0, t_f]. \tag{24}$$

The angular acceleration profile is bang-off-bang, as shown in Fig. 8

$$\ddot{\phi}(t) = u = \begin{cases} \ddot{\phi}_{max} & when\ t_0 \leq t \leq t_1, \\ 0 & when\ t_1 \leq t \leq t_2, \\ -\ddot{\phi}_{max} & when\ t_2 \leq t \leq t_f. \end{cases} \tag{25}$$

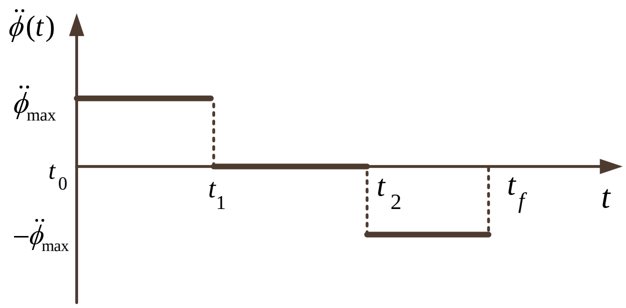

Figure 8. The optimal control law for case 1.

The angular velocity profile can be determined as

$$\dot{\phi}(t) = \begin{cases} \dot{\phi}_0 + \ddot{\phi}_{max}(t - t_0) & when\ t_0 \leq t \leq t_1, \\ \dot{\phi}_{max} & when\ t_1 \leq t \leq t_2, \\ \dot{\phi}_{max} - \ddot{\phi}_{max}(t - t_2) & when\ t_2 \leq t \leq t_f. \end{cases} \tag{26}$$

and he angular position can be find by direct integration of Eq. (26),

$$\phi(t) = \begin{cases} \dot{\phi}_0(t - t_0) + \frac{1}{2}\ddot{\phi}_{max}(t - t_0)^2 & when\ t_0 \leq t \leq t_1, \\ \phi(t_1) + \dot{\phi}_{max}(t - t_1) & when\ t_1 \leq t \leq t_2, \\ \phi(t_2) + \dot{\phi}_{max}(t - t_2) - \frac{1}{2}\ddot{\phi}_{max}(t - t_2)^2 & when\ t_2 \leq t \leq t_f. \end{cases} \tag{27}$$

Using the conditions, $\dot{\phi}(t_1) = \dot{\phi}_{max}$, $\dot{\phi}(t_f) = \dot{\phi}_f$, $\phi(t_f) = \phi_f$, we can determine switching times t_1, t_2, and final time t_f as:

$$t_1 = t_0 + \frac{\dot{\phi}_{max} - \dot{\phi}_0}{\ddot{\phi}_{max}}, \tag{28}$$

$$
\begin{aligned}
t_2 = & t_1 + \frac{1}{\dot{\phi}_{max}}\Big[\phi_f - \dot{\phi}_0(t_1 - t_0) - \frac{1}{2}\ddot{\phi}_{max}(t_1 - t_0)^2 \\
& - \frac{\dot{\phi}_{max}(\dot{\phi}_{max} - \dot{\phi}_f)}{\ddot{\phi}_{max}} + \frac{(\dot{\phi}_{max} - \dot{\phi}_f)^2}{2\ddot{\phi}_{max}}\Big],
\end{aligned} \tag{29}
$$

and

$$
t_f = t_1 + \frac{1}{\dot{\phi}_{max}}\Big[\phi_f - \dot{\phi}_0(t_1 - t_0) - \frac{1}{2}\ddot{\phi}_{max}(t_1 - t_0)^2 + \frac{(\dot{\phi}_{max} - \dot{\phi}_f)^2}{2\ddot{\phi}_{max}}\Big]. \tag{30}
$$

and the steering profiles including the quaternions, angular rate, and angular acceleration can be determined as

$$
{}^{\mathcal{N}}q^{\mathcal{T}}(t) = \Big[e_x \sin\frac{\phi(t)}{2}, e_y \sin\frac{\phi(t)}{2}, e_z \sin\frac{\phi(t)}{2}, \cos\frac{\phi(t)}{2}\Big]^T, \tag{31}
$$

$$
{}^{\mathcal{N}}\omega^{\mathcal{T}}(t) = \dot{\phi}(t)\hat{e}, \tag{32}
$$

$$
{}^{\mathcal{N}}\alpha^{\mathcal{T}}(t) = \ddot{\phi}(t)\hat{e}. \tag{33}
$$

Equations (25)–(33) can be used with proper boundary conditions to determine the steering laws for each segment of the SAS algorithm. This is shown in the next section for the acceleration constraint case.

Case 2: Single-Axis, Agile Slew Maneuver with Acceleration Constraint

Problem Statement: Consider the optimal control problem described by Eqs. (9), (10)–(12), subject to control constraint

$$
C_2 : \ |u = \ddot{\phi}| \leq \ddot{\phi}_{max}, \tag{34}
$$

and find ${}^{\mathcal{N}}\omega^{\mathcal{T}}$, ${}^{\mathcal{N}}\alpha^{\mathcal{T}}$, and ${}^{\mathcal{N}}q^{\mathcal{T}}$ for the SAS maneuver.

It is well known that the angular acceleration about the $\hat{e}$ axis is a bang-bang control as shown in Fig. 9.

$$
\ddot{\phi}(t) = \ddot{\phi}_{max}\mathbb{U}(t_0) - 2\ddot{\phi}_{max}\mathbb{U}(t - t_1), \tag{35}
$$

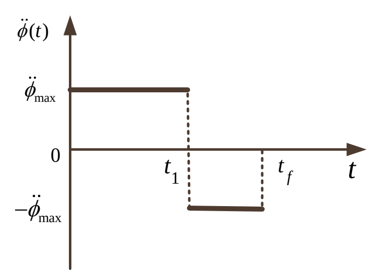

Figure 9. The optimal control in case 2.

where the switching and the final times are given by

$$
t_1 = t_0 - \frac{\dot{\phi}_0}{\ddot{\phi}_{max}} + \frac{\sqrt{\ddot{\phi}^2_{max}(2\ddot{\phi}_{max}\phi_f + \dot{\phi}^2_f + \dot{\phi}^2_0)}}{\sqrt{2}\ddot{\phi}^2_{max}}, \tag{36}
$$

and

$$t_f = t_0 - \frac{\dot{\phi}_f + \dot{\phi}_0}{\ddot{\phi}_{max}} + \frac{\sqrt{2}\sqrt{\ddot{\phi}_{max}^2(2\ddot{\phi}_{max}\phi_f + \dot{\phi}_{ef}^2 + \dot{\phi}_0^2)}}{\ddot{\phi}_{max}^2}. \tag{37}$$

The angular velocity and angular rate about the $\hat{e}$ axis are

$$\dot{\phi}(t) = \dot{\phi}_0 + \ddot{\phi}_{max}(t - t_0)\mathbb{U}(t_0) - 2\ddot{\phi}_{max}(t - t_1)\mathbb{U}(t - t_1), \tag{38}$$

$$\phi(t) = \dot{\phi}_0(t - t_0) + \ddot{\phi}_{max}\frac{(t - t_0)^2}{2}\mathbb{U}(t_0) - 2\ddot{\phi}_{max}\frac{(t - t_1)^2}{2}\mathbb{U}(t - t_1). \tag{39}$$

The First Slew Maneuver: This is a single-axis nonrest-to-rest maneuver around the $\hat{e}$ with boundary conditions,

$$\dot{\phi}(t_0) = \dot{\phi}_0, \phi(t_0) = 0, \dot{\phi}(t_{f1}) = 0, \phi(t_{f1}) = \phi_1. \tag{40}$$

The switching time, t_{11}, and the minimum-time, t_{f1}, are

$$t_{11} = t_0 - \frac{\dot{\phi}_0}{\ddot{\phi}_{max}} + \frac{\sqrt{\ddot{\phi}_{max}^2(2\ddot{\phi}_{max}\phi_1 + \dot{\phi}_0^2)}}{\sqrt{2}\ddot{\phi}_{max}^2}, \tag{41}$$

$$t_{f1} = t_0 - \frac{\dot{\phi}_0}{\ddot{\phi}_{max}} + \frac{\sqrt{2\ddot{\phi}_{max}^2(2\ddot{\phi}_{max}\phi_1 + \dot{\phi}_0^2)}}{\ddot{\phi}_{max}^2}. \tag{42}$$

The Second Slew Maneuver: This is a rest-to-rest maneuver around the sun vector with boundary conditions given by

$$\dot{\phi}(t_0) = 0, \phi(t_0) = 0, \dot{\phi}(t_{f2}) = 0, \phi(t_{f2}) = \phi_2. \tag{43}$$

The switching time, t_{12}, and the minimum-time, t_{f2}, are

$$t_{12} = t_0 - \frac{\sqrt{\phi_2}}{\ddot{\phi}_{max}}, \tag{44}$$

$$t_{f2} = t_0 - \frac{2\sqrt{\phi_2}}{\ddot{\phi}_{max}}. \tag{45}$$

The Third Slew Maneuver: This is a single-axis rest-to-nonrest maneuver around the $\hat{e}$ with boundary conditions,

$$\dot{\phi}(t_0) = 0, \phi(t_0) = 0, \dot{\phi}(t_{f3}) = \dot{\phi}_f, \phi(t_{f3}) = \phi_3. \tag{46}$$

The switching time, t_{13}, and the minimum-time, t_{f3}, are

$$t_{13} = t_0 + \frac{\sqrt{\ddot{\phi}_{max}^2(2\ddot{\phi}_{max}\phi_3 + \dot{\phi}_f^2)}}{\sqrt{2}\ddot{\phi}_{max}^2}, \tag{47}$$

$$t_{f3} = t_0 - \frac{\dot{\phi}_f}{\ddot{\phi}_{max}} + \frac{\sqrt{2\ddot{\phi}_{max}^2(2\ddot{\phi}_{max}\phi_3 + \dot{\phi}_f^2)}}{\ddot{\phi}_{max}^2}. \tag{48}$$

Knowing the switching time for each slew, the $\ddot{\phi}(t)$, $\dot{\phi}(t)$, and $\phi(t)$, can be found by substituting the boundary conditions for each slew in to Eqs. (35), (38), and (39), respectively. Then the steering laws, i.e. ${}^{\mathcal{N}}\omega^{\mathcal{T}}(t)$, ${}^{\mathcal{N}}\alpha^{\mathcal{T}}(t)$, ${}^{\mathcal{N}}q^{\mathcal{T}}(t)$, can be found from Eqs. (31)–(33).

NUMERICAL SIMULATION

CONCLUSION

ACKNOWLEDGMENT

NOTATION

$\mathcal{G}$-frame	gyrostat body-fixed frame
${}^{\mathcal{N}}H^{\mathcal{G}/\mathcal{G}*}$	the total angular momentum of the gyrostat with respect to its center of mass
$I^{\mathcal{G}/\mathcal{G}^*}$	the mass-moment-of-inertia of the gyrostat
$I^{w/w*}$	the mass-moment-of-inertia of reaction wheels with respect to their center of masses
M_{max}	the maximum available torque along the eigenaxis
$\mathcal{N}$-frame	the Newtonian frame
${}_{\mathcal{G}}\hat{P}$	unit vector along the bore sight of payload in the $\mathcal{G}$-frame
${}_{\mathcal{N}}\hat{P}_i$	unit vector of the initial point in the $\mathcal{N}$-frame
${}_{\mathcal{N}}\hat{P}_f$	unit vector of the final point in the $\mathcal{N}$-frame
${}^{\mathcal{N}}q^{\mathcal{T}}$	quaternion of the $\mathcal{T}$-frame in the $\mathcal{N}$-frame
${}_{\mathcal{N}}\hat{S}$	unit vector of the sun vector in the $\mathcal{N}$-frame
$\mathcal{T}$-frame	the target frame
ϵ_p	Payload half-cone angle
${}^{\mathcal{N}}\alpha^{\mathcal{T}}$	angular acceleration of the $\mathcal{T}$-frame in the $\mathcal{N}$-frame
${}^{\mathcal{N}}\omega^{\mathcal{T}}$	angular velocity of the $\mathcal{T}$-frame in the $\mathcal{N}$-frame

REFERENCES

[1] C. R. McInnes, "Large angle slew maneuvers with autonomous sun vector avoidance," *Journal of Guidance Control Dynamics*, Vol. 17, 06 1994, pp. 875–877, 10.2514/3.21283.

[2] K. Spindler, "New Methods in On-Board Attitude Control (AAS 98-308)," Vol. 100, 01 1998.

[3] H. B. Hablani, "Attitude commands avoiding bright objects and maintaining communication with ground station," *Advances in the Astronautical Sciences*, 1998, 10.2514/2.4469.

[4] J. D. Biggs and L. Colley, "Geometric Attitude Motion Planning for Spacecraft with Pointing and Actuator Constraints," *Journal of Guidance, Control, and Dynamics*, 2016, 10.2514/1.G001514.

[5] E. Frazzoli, M. A. Dahleh, E. Feron, R. P. Kornfeld, and R. P. Kornfeld, "A Randomized Attitude Slew Planning Algorithm for Autonomous Spacecraft," *In AIAA Guidance, Navigation, and Control Conference*, 2001.

[6] D. Spiller, L. Ansalone, and F. Curti, "Particle Swarm Optimization for Time-Optimal Spacecraft Reorientation with Keep-Out Cones," *Journal of Guidance, Control, and Dynamics*, 2016, 10.2514/1.G001228.

[7] Y. Kim and M. Mesbahi, "Quadratically constrained attitude control via semidefinite programming," *IEEE Transactions on Automatic Control*, 2004, 10.1109/TAC.2004.825959.

[8] Y. Kim, M. Mesbahi, G. Singh, and F. Y. Hadaegh, "On the convex parameterization of constrained spacecraft reorientation," *IEEE Transactions on Aerospace and Electronic Systems*, 2010, 10.1109/TAES.2010.5545176.

[9] C. Sun and R. Dai, “Spacecraft Attitude Control under Constrained Zones via Quadratically Constrained Quadratic Programming,” 2015, 10.2514/6.2015-2010.

[10] U. Lee and M. Mesbahi, “Quaternion based optimal spacecraft reorientation under complex attitude constrained zones,” *Advances in the Astronautical Sciences*, 2014.

[11] M. Diaz Ramos and H. Schaub, “Kinematic Steering Law for Conically Constrained Torque-Limited Spacecraft Attitude Control,” *Journal of Guidance, Control, and Dynamics*, Vol. 41, jul 2018, pp. 1990–2001, 10.2514/1.G002873.